

Supporting information for

Amphiphilic Modification and Asymmetric Silica Encapsulation of Dumbbell-like Au-Fe₃O₄ Nanoparticles

Binghui Wu, Shaoheng Tang, Mei Chen, and Nanfeng Zheng*

State Key Laboratory for Physical Chemistry of Solid Surfaces, Collaborative Innovation Center of Chemistry for Energy Materials, and Department of Chemistry, College of Chemistry and Chemical Engineering, Xiamen University, Xiamen 361005, China

Email: nfzheng@xmu.edu.cn

Experimental Details

Reagents: All syntheses were carried out using commercially available reagents. HAuCl₄·4H₂O (Au content: ≥47.8%), *n*-hexane (97%), cyclohexane (99.5%), *n*-octane (99.7%), 4-Nitrophenol (≥99%), NaBH₄ (>96%) and ethanol (≥99.7%) were purchased from Sinopharm Chemical Reagent Co., Ltd. *Tert*-butylamine-borane complex (TBAB, 95%), Iron(III) acetylacetonate (Fe(acac)₃, 99%), oleylamine (OAm, C18 content: 80%-90%), and 1-Dodecanethiol (C₁₂SH, ≥98.5%) were purchased from Acros Organics. Oleic acid (OLA, 90%), Brij[®]C10 (C₁₆H₃₃(OCH₂CH₂)_nOH, n≈10), fluorescein isothiocyanate (FITC), 3-aminopropyltriethoxysilane (APTES) and Trimethoxy(octadecyl)silane (90%) were purchased from Sigma Aldrich. Tetraethylorthosilicate (TEOS, >99%) was purchased from Alfa Aesar. Ammonia solution (25-28% wt) was purchased from Guangdong Guanghua Sci-Tech co., Ltd. N₂ (99.999%) was purchased from Linde Gas. RPMI 1640 cell culture medium was purchased from Hyclone Laboratories Inc. HeLa cells were purchased from cell storeroom of Chinese Academy of Science. The water used in all experiments was ultrapure. All other chemicals were used as received without further purification.

Synthesis of OAm-capped Au nanoparticles: Monodisperse Au nanoparticles were synthesized according to our previous report.^{S1} In the synthesis of 8.1±0.5 nm Au nanoparticles, an orange precursor solution of *n*-octane (10 mL), OAm (10 mL), and HAuCl₄·4H₂O (0.25 mmol) was prepared in air at 15 °C thermostatic bath and

magnetically stirred under N₂ flow (~30 mL/min) for 10 min. A reducing solution containing TBAB (0.167 mmol), *n*-octane (1 mL), and OAm (1 mL) was mixed by sonication, cooled to 15 °C and then injected into the precursor solution. (To get 8.1 nm Au nanoparticles, the exact amount of TBAB may be dependent on the companies which TBAB purchased from, but the monodispersity remains in the linear solvent^{S1}.) The reduction reaction was slowly initiated and the solution changed to a deep purple color within 20 s. The mixture was allowed to react at 15 °C for 1 h before ethanol (60 mL) was added to precipitate the Au NPs. The Au NPs were collected by centrifugation (6,000 rpm, 5 min), washed with ethanol and redispersed in hexane to form a stock solution (~5 mg/mL).

Synthesis of Au-Fe₃O₄ dumbbell nanoparticles by microwave heating: The dumbbell nanoparticles were synthesized according to a modified method that was described previously.^{S2} 0.4 mL hexane solution containing 2 mg 8.1 nm Au nanoparticles, 15 mg Fe(acac)₃ and 2 mL OAm were mixed together in a 10-mL microwave vial. The vial was kept open and directly dipped into oil bath which was preheated to 130 °C and stirred in air for 30 min to evaporate hexane and dissolve Fe(acac)₃. After the mixture was cooled to room temperature, OLA (1 mL) was added. The vessel was then sealed before microwave irradiation. The microwave reaction was carried out in a focused single-mode microwave synthesis system (Discover, CEM, USA). The mixture was pre-stirred for 2 min and then heated to 120 °C by 50 W of microwave radiation with stirring. After keeping at this temperature for 15 min, the mixture was further heated to 180 °C by 100 W with stirring and aged for another 15 min. After cooling to room temperature, the particles were separated by adding ethanol, collected by a permanent magnet, and redispersed into cyclohexane.

Synthesis of Au-(Fe₃O₄@SiO₂) nanoparticles with Au exposed in reversed micelles: The OAm/OLA-capped Au-Fe₃O₄ nanoparticles (containing 2 mg Au) were collected by the magnet and free from ethanol treatment (i.e., just remove the excess OAm and OLA), and added into the mixture of 0.5 mL dodecanethiol and 6 mL of cyclohexane. The mixture was stirred overnight at 35 °C. Then another 6 mL of

cyclohexane, 2.73 g of Brij[®]C10 and 0.1 mL of NH₃·H₂O was added. After stirring at 35 °C for 1 h, 100 μL of TEOS was added and the mixture was further stirred at 50 °C for 5 h. The products were collected by a permanent magnet and washed with mixture of water and ethanol (1:8) for five times. (The obtained Au-(Fe₃O₄@SiO₂) nanoparticles can be dispersed in the pure phase of water other than oil-water interface, due to the relatively low coverage of thiol in the view of total surface of each nanoparticle. Besides Brij[®]C10, Igepal[®]CO-520 can also be used for the (asymmetric) silica encapsulation but the reaction was performed at room temperature.^{S3}) **(Au-Fe₃O₄)@SiO₂ nanoparticles**, with Au-Fe₃O₄ dimers completely encapsulated, were synthesized under the similar condition above, but without adding any thiol.

Synthesis of FITC-doped Au-(Fe₃O₄@SiO₂) or (Au-Fe₃O₄)@SiO₂ nanoparticles:

2 mg of FITC was reacted with 15 μL of APTES in 1 mL of ethanol under dark conditions for 8 h. The prepared FITC–APTES stock solution was kept at 4 °C. To synthesize Au-(Fe₃O₄@SiO₂) or (Au-Fe₃O₄)@SiO₂ nanoparticles doped with FITC, the synthetic process was similar to that of pure Au-(Fe₃O₄@SiO₂) or (Au-Fe₃O₄)@SiO₂ nanoparticles, except that 50 μL of FITC–APTES stock solution was injected into the reverse micelles after injecting 100 μL of TEOS. The shape of Au-(Fe₃O₄@SiO₂) or (Au-Fe₃O₄)@SiO₂ nanoparticles remained unchanged upon FITC doping.

Amphiphilic modification of hydrophobic Au-Fe₃O₄ nanoparticles at planar

oil-water interface: The OAm/OLA-capped Au-Fe₃O₄ nanoparticles obtained by microwave heating were precipitated by ethanol, collected by a permanent magnet, and added into the mixture of dodecanethiol (0.5 mL) and cyclohexane (20 mL). After stirring for 0.5 hour, 30 mL ice ammonia water was added. After intense stirring for one day, Au-Fe₃O₄ nanoparticles were collected into the interface between cyclohexane and water. (It is possible to only take 1 hour for the ligand exchange,

however, to ensure that each Au-Fe₃O₄ nanoparticle becomes amphiphilic, more time (24 hours) is used here.) The water phase and oil phase were carefully replaced by clean water and cyclohexane, respectively. The resulting Au-Fe₃O₄ nanoparticles are amphiphilic and ready for further research.

Synthesis of amphiphilic Au-Fe₃O₄/SiO₂ nanofilm: A appropriate amount of amphiphilic Au-Fe₃O₄ nanoparticles were added into the interface of cyclohexane and ice ammonia water (v/v, 1:1) until there was no obvious wrinkle or aggregation at the interface. Then TEOS was added into the oil phase (the total amount of TEOS is dependent on the area of the interface, ~15-20 μL/cm²), and the vessel was undisturbedly placed for 3 days. The vessel could be a round flask hermetically sealed with Parafilm or a bottle with a cover to prevent NH₃ and cyclohexane from escaping.

Silanization of glass slide: A clean and transparent glass slide (76.2×25.4×1.2 mm) was put into a mixture solution of 80 mL ethanol, 0.3 mL trimethoxy(octadecyl)silane and 1 mL ammonia water, and magnetically stirred at 50 °C thermostatic bath for one day. Then the milky white semitransparent glass slide was washed with water and ethanol and wiped with tissue paper. Finally, the glass turned transparent again but hydrophobic.

Loading amphiphilic Au-Fe₃O₄/SiO₂ nanofilm on glass slide: To get the hydrophobic surface of the Au-Fe₃O₄/SiO₂ nanofilm, a hydrophilic glass slide was put into the water phase before synthesis of the Au-Fe₃O₄/SiO₂ nanofilm. After the film was formed three days later, the cyclohexane phase was replaced with clean cyclohexane, then the glass slide was lifted horizontally or obliquely (bottom-lifting technique) and dried for contact angle test.^{S4} To get hydrophilic surface of the Au-Fe₃O₄/SiO₂ nanofilm, the cyclohexane phase was replaced with clean cyclohexane and then evaporated to let the Au-Fe₃O₄/SiO₂ nanofilm stay at the air-water interface. After that, a hydrophobic glass slide was horizontally stucked against the interface from above, then lifted vertically (top-lifting technique) and dried for contact angle test.^{S4}

Characterization:

Transmission electron microscopy (TEM): TEM studies were performed on TECNAI F-30 high-resolution transmission electron microscopy operating at 300 kV. The samples dispersed in a homogeneous solvent were prepared by dropping dispersion of samples onto 300-mesh carbon-coated copper grids and by immediately evaporating the solvent at room temperature. The samples dispersed at the oil-water interface were fished up and attached to a copper grid assisted by a tweezer while letting the samples dry at room temperature.

Catalytic reduction of 4-Nitrophenol: An Au-(Fe₃O₄@SiO₂) or (Au-Fe₃O₄)@SiO₂ suspension in water (0.40 mL, 6.25×10⁻⁵ M with respect to the gold precursor concentration) was added to NaBH₄ aqueous solution (1 mL, 1.2 M). 4-Nitrophenol (1 mL, 6.8×10⁻³ M) was then added to the mixture, which was stirred until the deep yellow solution became colorless. During the course of reaction, samples were withdrawn at regular intervals (3 min) and measured by UV-vis absorption spectra.^{S5}

Contact angle measurements: The water-repellent properties of water droplets on the sample surfaces were characterized using an optical contact-angle meter system (KRÜSS, DSA100, Germany). The droplets used for the CA measurement were 4 mg. Before contact angle test, the Au-Fe₃O₄/SiO₂ nanofilm was transferred onto hydrophilic and hydrophobic glass slides by bottom-lifting and top-lifting technique, respectively.^{S4}

Fluorescence imaging and flow cytometry analysis: HeLa cells were plated in 24 well-plate with a density of 5×10⁴ cells per well. After incubation in the fresh RPMI 1640 medium for 24 h, HeLa cells were incubated separately with 0.5 mL of media containing the FITC-modified Au-(Fe₃O₄@SiO₂) or FITC-modified (Au-Fe₃O₄)@SiO₂ samples in the same concentration (20 µg/mL in Au, or ~300 µg/mL in all). After 8-h incubation, the media were removed. The cells were carefully washed for 5 times by phosphate buffer solution (PBS). Then the cells on the plate were directly used for **fluorescence imaging** to detect the green fluorescence emission in cells under the fluorescence microscopy. For **flow cytometry**, the adherent cells were detached from the plate by treatment with trypsin-EDTA, washed and then suspended in 0.5 mL PBS buffer solution for flow cytometry.

Size distribution and Zeta potential: Size distribution and Zeta potential

experiments were carried out on a Nano-ZS (Malvern Instruments), using ultrapure water as solvent.

MRI Phantom Study: The phantom study was performed on a 0.5 T NMI20-Analyst NMR Analyzing&Imaging system (Niumag Corporation, Shanghai, China). The samples for MRI phantom study were prepared separately. Au-(Fe₃O₄@SiO₂) nanoparticles were prepared with concentrations of 400, 200, 100, 50, 25, and 12.5 μM of Fe ions in 1% agarose-containing solution. The control sample denoted as 0 μM was prepared with purified water containing 1% agarose. The transverse relaxation times were measured (at 300 K). *T*₂-weighted MR images of all the samples were acquired under the following parameters: TR/TE= 2000/80 ms, 256×128 matrices, repetition times = 4.

***In vitro* Computed Tomography Imaging:** Computed tomography (CT) imaging was acquired using a Mediso nanoScan SPECT/CT scanner. Imaging parameters were as follows: slice thickness, medium; tube energy, 50 kVp, 670 μA; CTDIvol, 1881.6 cGy; DLP, 51800.0 cGy×mm; semicircular parameters, full scan; number of projections, 480; In-plane voxel size, medium. CT data were analyzed using the Hounsfield units (HU) for regions.

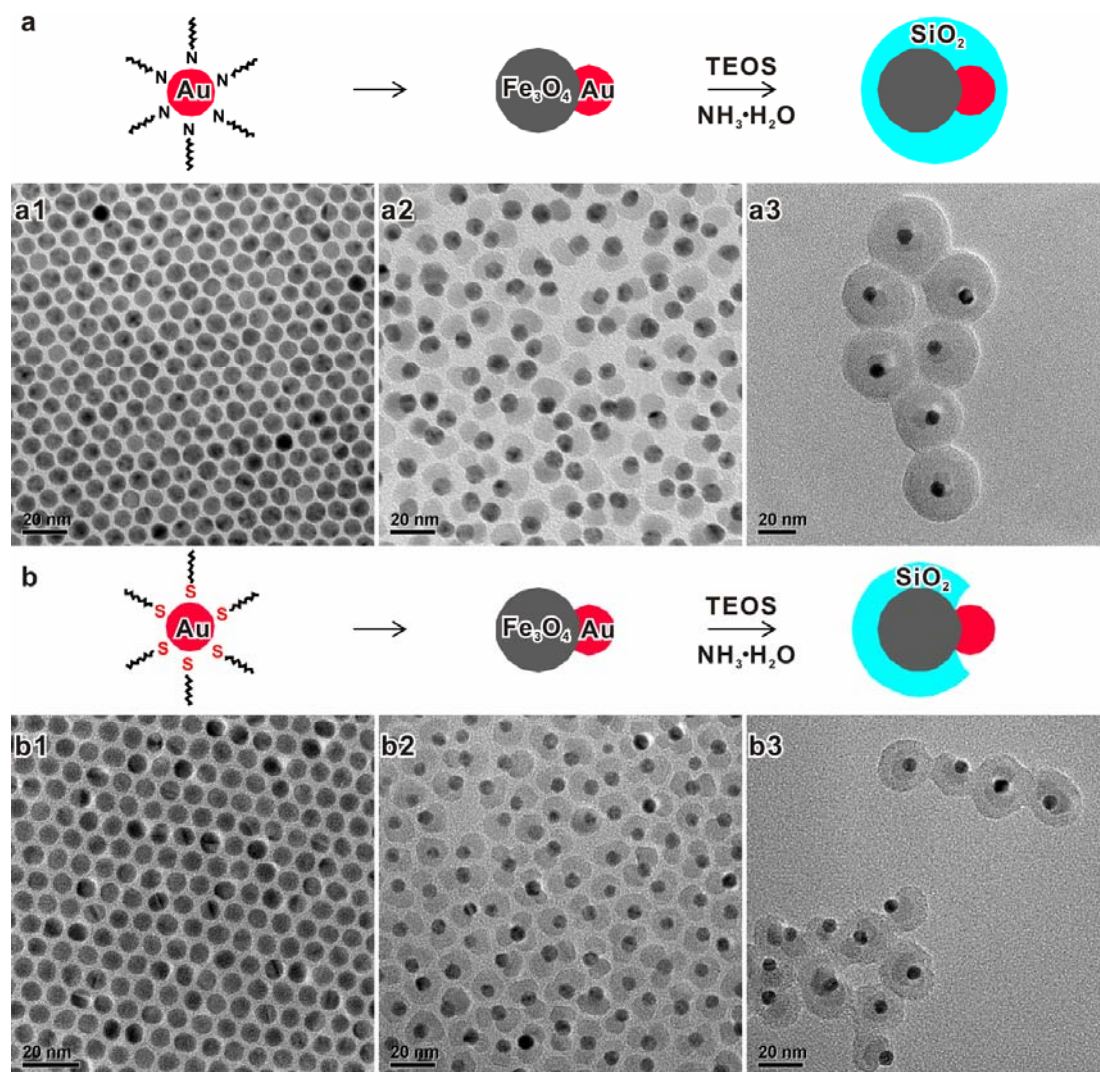


Figure S1. (a) Schematic diagram of the generation of (Au-Fe₃O₄)@SiO₂ nanoparticles, starting from OAm-capped Au nanoparticle and then complete silica encapsulation; (a1-3) corresponding TEM images of 8.1±0.5-nm OAm-capped Au (synthesized according to the previous report),^{S1} Au-Fe₃O₄ and (Au-Fe₃O₄)@SiO₂. (b) Schematic diagram of the generation of Au-(Fe₃O₄@SiO₂) nanoparticles, starting from thiol-capped Au nanoparticle and then asymmetric silica encapsulation; (b1-3) corresponding TEM images of 6.9±0.3-nm C₁₂SH-capped Au (synthesized according to the previous report),^{S6} Au-Fe₃O₄ and Au-(Fe₃O₄@SiO₂).

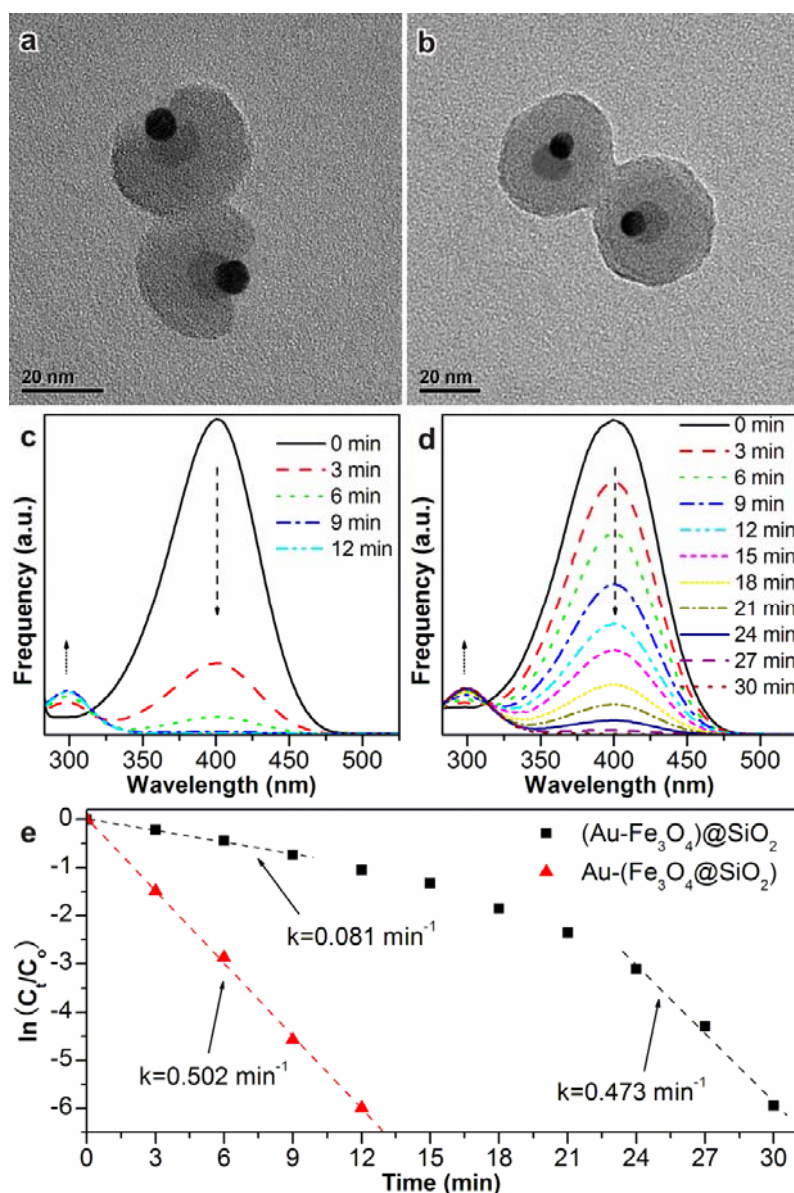


Figure S2. (a,b) Magnified TEM images of Au-(Fe₃O₄)@SiO₂ and (Au-Fe₃O₄)@SiO₂, respectively. (c,d) The time-domain UV-vis spectra of the reaction mixture during the reduction process of 4-nitrophenol in aqueous solution of NaBH₄ catalyzed by (a) Au-(Fe₃O₄)@SiO₂ and (b) (Au-Fe₃O₄)@SiO₂, respectively. The arrows indicate the increase of reaction time. (e) The linear relationship between ln(C_t/C₀) and reaction time during the reduction process of 4-nitrophenol. The totally encapsulated (Au-Fe₃O₄)@SiO₂ nanoparticles shouldn't have showed catalytic activity due to no access of Au, however, here they exhibited an increasing activity during the catalysis, mainly due to spontaneous morphology change from solid to hollow spheres resulting from NaBH₄ etching and final exposure of Au nanoparticles (Figure S3).

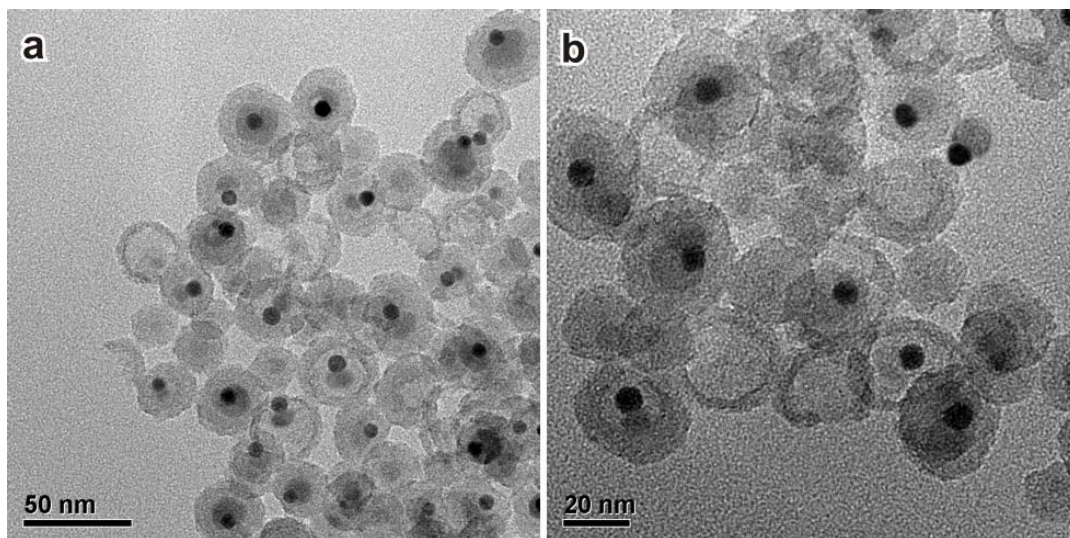


Figure S3. (a,b) TEM images of the $(\text{Au-Fe}_3\text{O}_4)@\text{SiO}_2$ collected after reduction of 4-nitrophenol using NaBH_4 as reducing agent. It has been reported that silica colloids can be spontaneously transformed from solid spheres to hollow structures in aqueous solutions of NaBH_4 .^{S7}

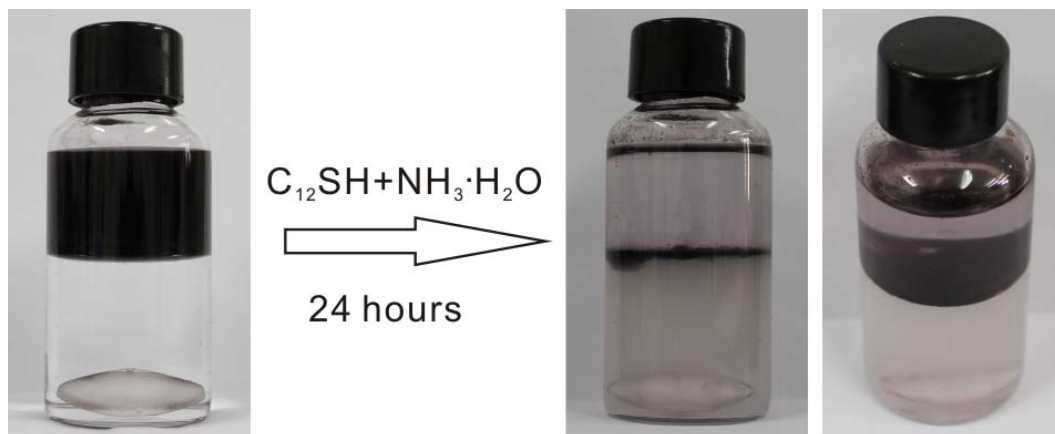


Figure S4. Photographs of the mixture of OAm/OLA-capped $\text{Au-Fe}_3\text{O}_4$ nanoparticles, cyclohexane, dodecanethiol and ammonia solution before and after vigorous stirring.

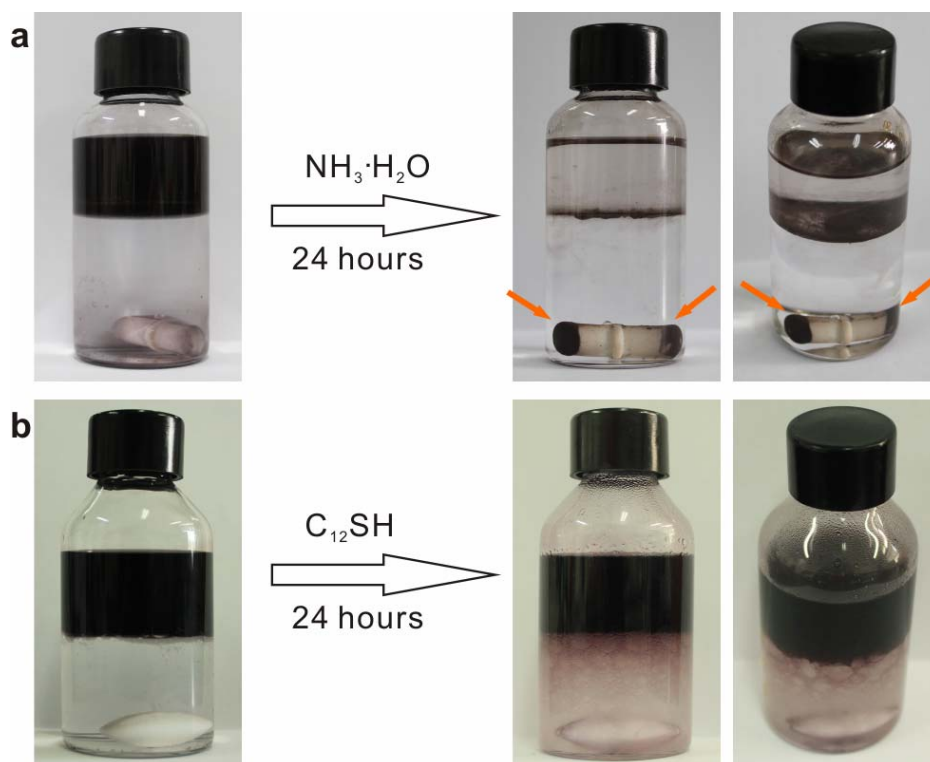


Figure S5. Photos of (a) mixture of Au-Fe₃O₄, cyclohexane and ammonia water (without C₁₂SH), (b) mixture of Au-Fe₃O₄, cyclohexane, C₁₂SH and water (without ammonia) before and after intense stirring for 24 h. The orange arrow in (a) indicates the hydrophilic Au-Fe₃O₄ nanoparticles adsorbed on both ends of a magnet.

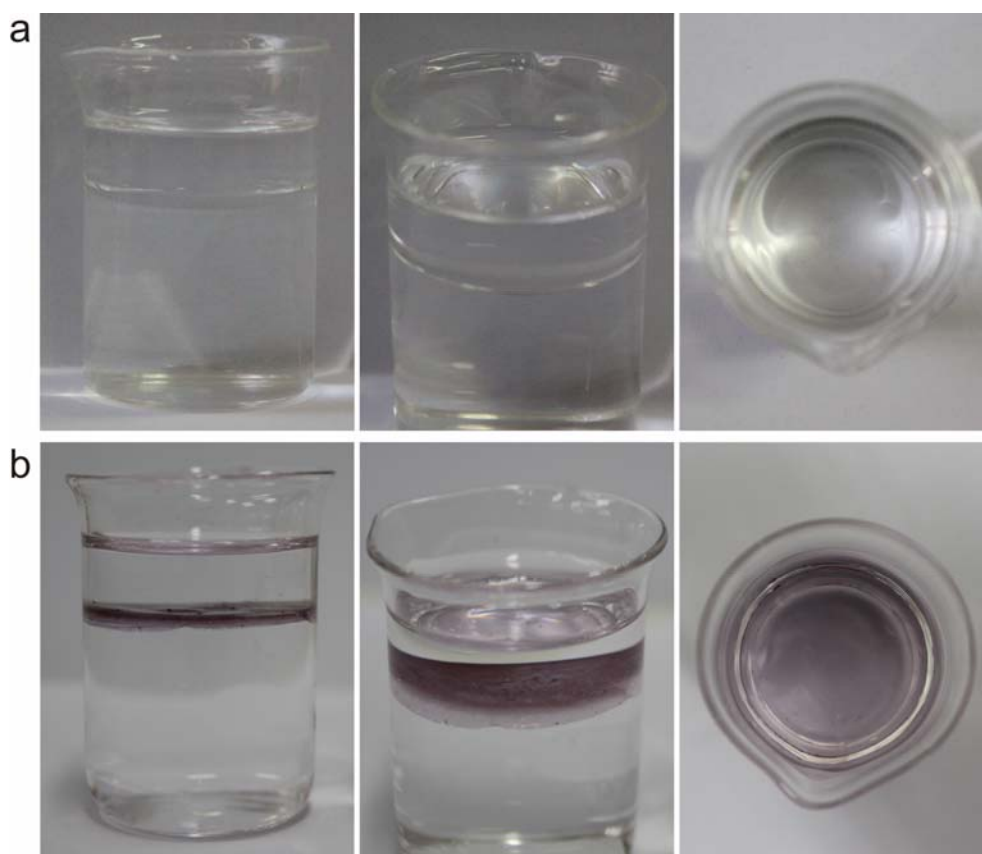


Figure S6. Photos of mixture of cyclohexane and water (a) before and (b) after adding a small amount of amphiphilic Au-Fe₃O₄ dumbbell nanoparticles pretreated by thiol and ammonia shown in Figure S4. Amphiphilic Janus Au-Fe₃O₄ nanoparticles are easy to form a close-packed monolayer at the water-cyclohexane interface with a visible gold mirror reflectance (metallic sheen).

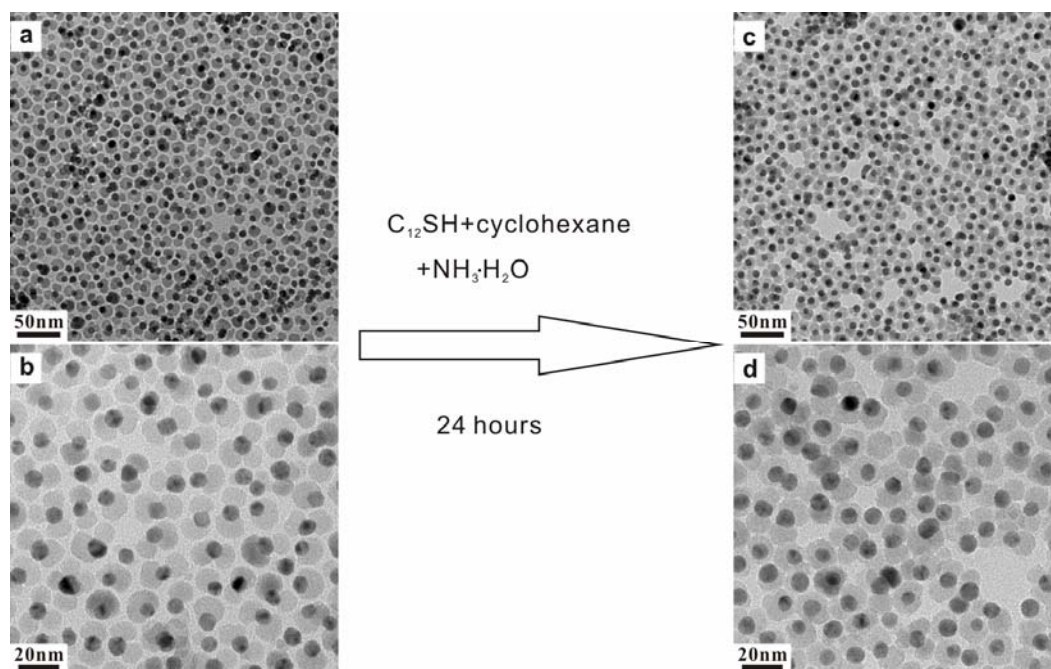


Figure S7. (a,b) TEM images of OAm/OLA-capped Au-Fe₃O₄ nanoparticles. (c,d) TEM images of amphiphilic Au-Fe₃O₄ nanoparticles collected from the oil-water interface shown in Figure S6b.

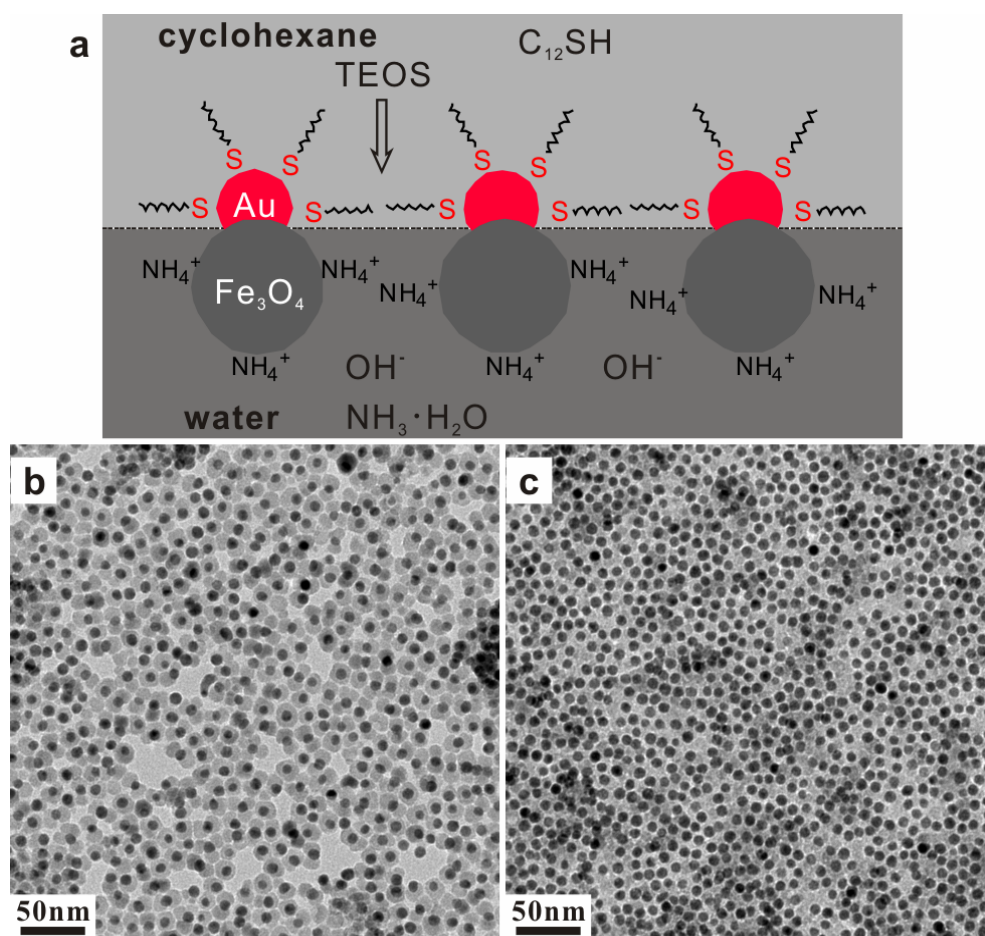


Figure S8. (a) Schematic diagram of the generation of an Au-Fe₃O₄/SiO₂ nanofilm at the planar oil-water interface. (b) TEM image of amphiphilic Au-Fe₃O₄ monolayer after treatment by thiol and ammonia. (c) TEM image of the resulted Au-Fe₃O₄/SiO₂ nanofilm grown in the way of (a), using amphiphilic Au-Fe₃O₄ monolayer shown in (b) as seeds. The maximal number density of hexagonal close packing of 8.1 nm Au was calculated as 110 particles per 100 nm × 100 nm based on Figure 1b. The number density of Au nanoparticles on the amphiphilic Au-Fe₃O₄ monolayer and Au-Fe₃O₄/SiO₂ nanofilm is about 65 and 73 particles per 100 nm × 100 nm, respectively (Figure S8b-c). A slight increase of the number density of Au nanoparticles on Au-Fe₃O₄/SiO₂ nanofilm compared to that on amphiphilic Au-Fe₃O₄ monolayer may be due to the elimination of surface charge repulsion and the crosslink in the hydrolysis and condensation process of TEOS.

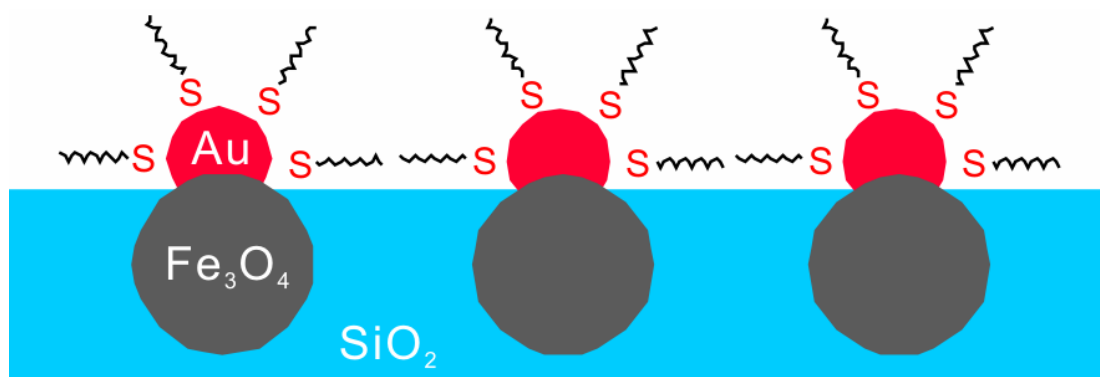


Figure S9. Schematic diagram of amphiphilic Au-Fe₃O₄/SiO₂ nanofilm.

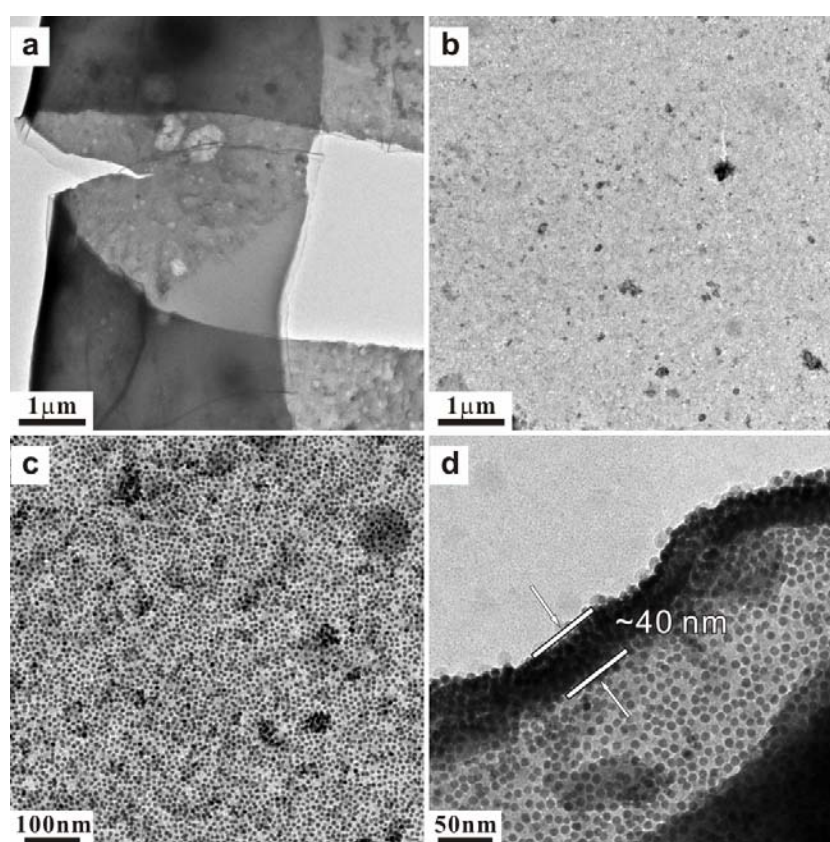


Figure S10. TEM images of Au-Fe₃O₄/SiO₂ nanofilms on TEM carbon support film: (a) a fractured nanofilm, (b) low- and (c) high- magnification of a plane nanofilm, (d) a curled nanofilm. EDS spectrum (Figure S11) confirmed that the as-prepared nanofilm contained SiO₂.

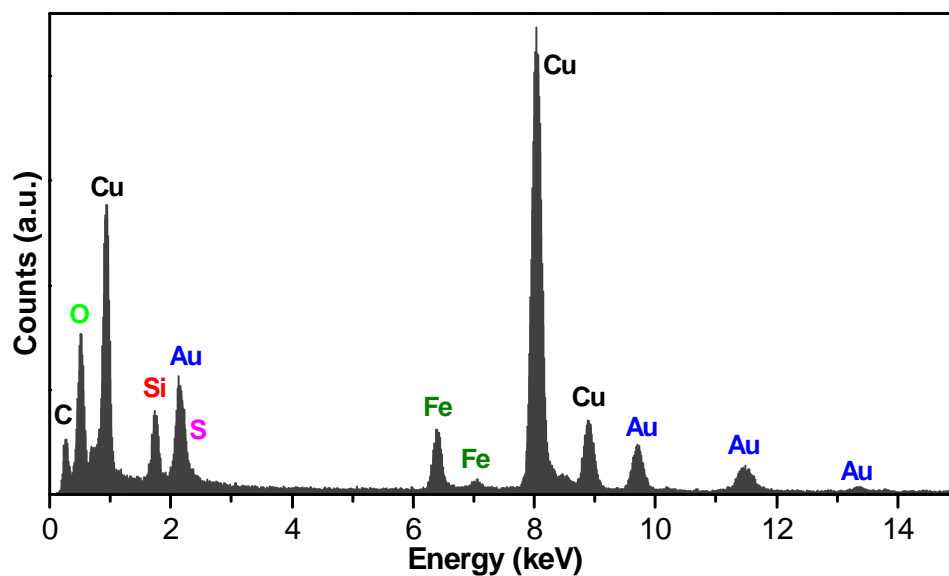


Figure S11. The EDS spectrum of the Au-Fe₃O₄/SiO₂ nanofilms on carbon-coated copper grid. It should be pointed out that it is hard to differentiate S (right) from Au (left) at 2.1-2.3 keV, because EDS peak of S is closed to that of Au and the content of S is much less than that of Au.

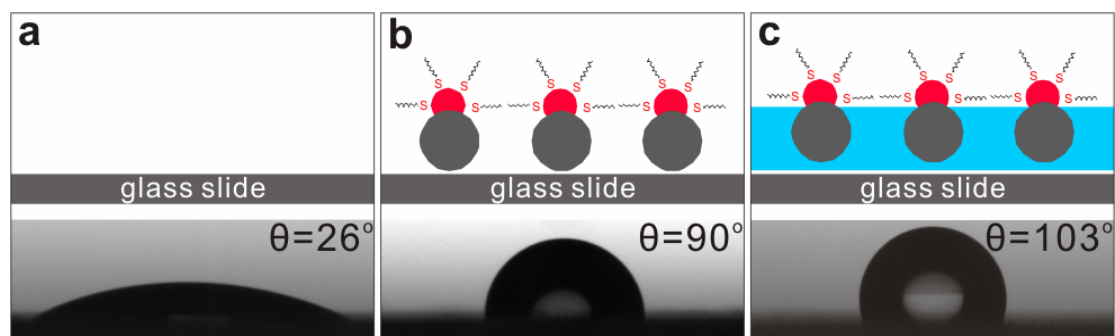


Figure S12. Photographs of a water droplet deposited on various surfaces: (a) clean glass slide, (b) hydrophilic glass slide covered with a monolayer of close-packing amphiphilic Au-Fe₃O₄ nanoparticles, (c) hydrophilic glass slide covered with amphiphilic Au-Fe₃O₄/SiO₂ nanofilm. For comparison, the wettability of both the clean glass slide and amphiphilic Au-Fe₃O₄ monolayer on glass slide was tested first. It is known that contact angle of 65° has been defined as the boundary between hydrophilicity and hydrophobicity on the basis of differences in the structure of interfacial water.^{S8-9} As shown in Figure S12a-b, the amphiphilic Au-Fe₃O₄ monolayer on clean glass slide was hydrophobic with a contact angle of 90±3°. This result indicates that the hydrophilic Fe₃O₄ segment of the amphiphilic Au-Fe₃O₄ monolayer prefers to adhere to the surface of hydrophilic glass slide, leaving the hydrophobic segment (Au nanoparticles) exposed to air. When transferred on a hydrophilic glass slide, the Au-Fe₃O₄/SiO₂ nanofilm gave an even higher water contact angle of 103±3° (Figure S12c), which can be explained by the larger number density of hydrophobic Au nanoparticles as discussed above (Figure S8b-c).

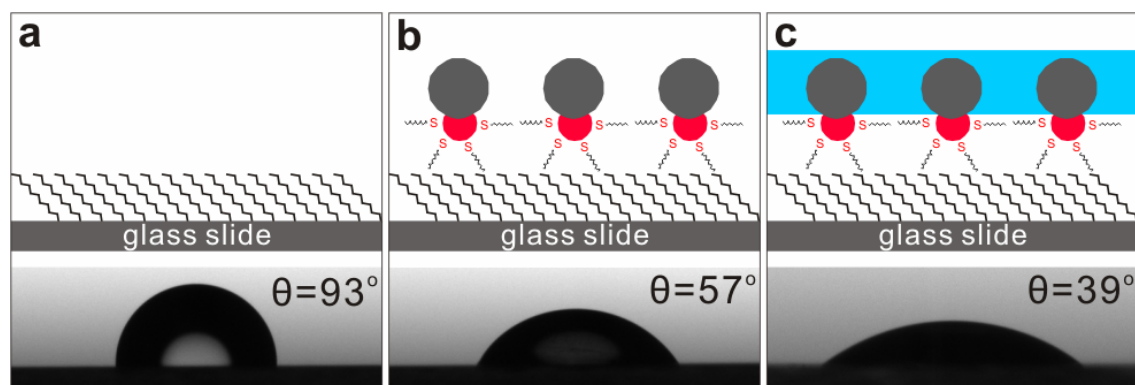


Figure S13. Photos of a water droplet deposited on varied surfaces: (a) hydrophobic glass slide created by the silanization of the silica slide surface with trimethoxy(octadecyl)silane, (b) hydrophobic glass slide covered with a monolayer of close-packing amphiphilic Au-Fe₃O₄ nanoparticles, (c) hydrophobic glass slide covered with amphiphilic Au-Fe₃O₄/SiO₂ film. The water contact angle of surface shown in (b) was not so hydrophilic, and it was dependent on the chemical functionality of the underlying substrate, suggesting that Janus Au-Fe₃O₄ nanoparticles were asymmetrically functionalized with thiol and NH₃ ligands.^{S10}. Figure S13c indicates that the hydrophobic surface of Au-Fe₃O₄/SiO₂ nanofilm can also adhere to hydrophobic glass slide, leading to the exposure of hydrophilic surface to air.

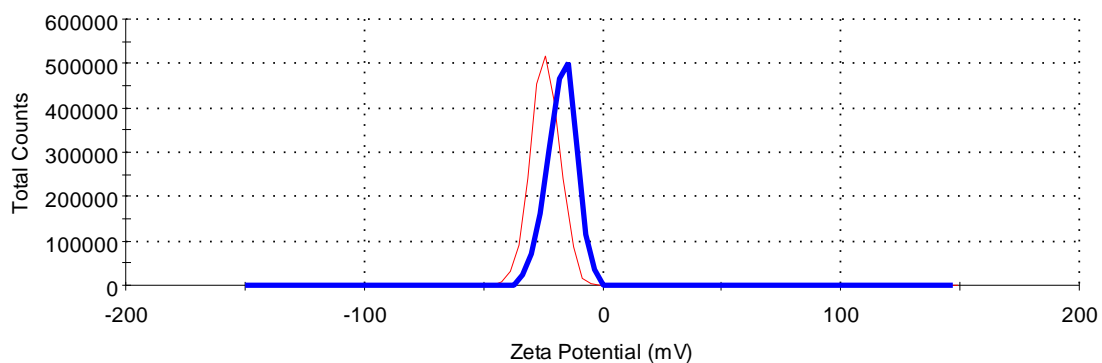


Figure S14. Zeta potentials of FITC-modified (—) Au-(Fe₃O₄@SiO₂) and (—) (Au-Fe₃O₄)@SiO₂ in water; the average values of Zeta potentials are -23.9 and -17.1 mV, respectively.

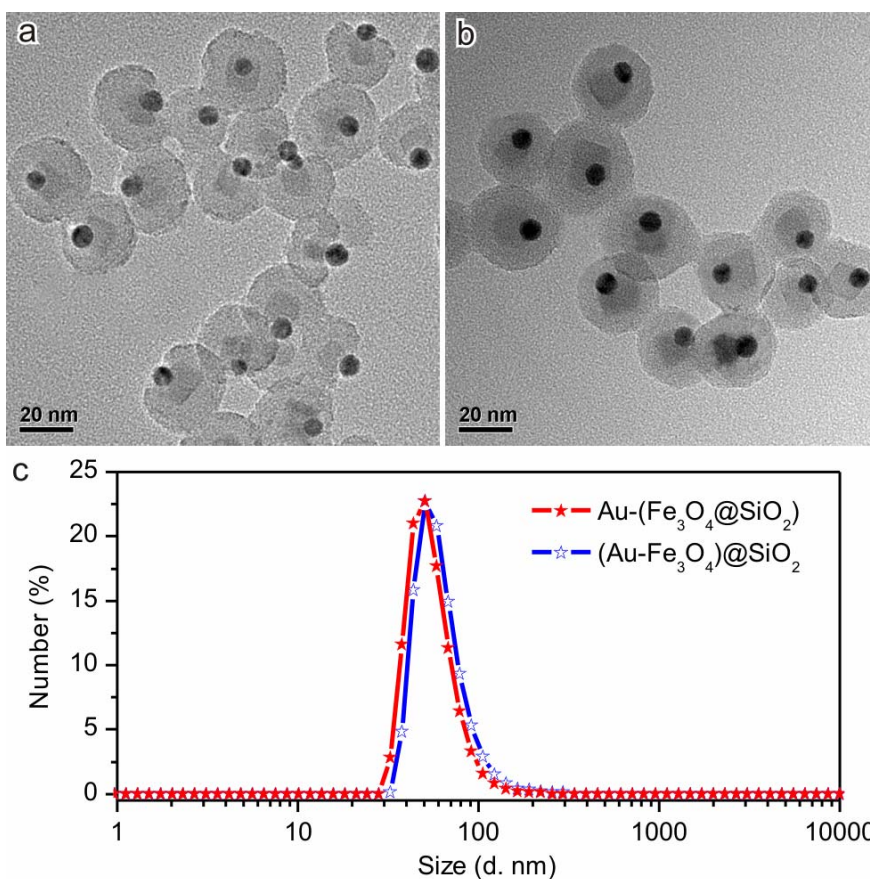


Figure S15. TEM images of FITC-modified (a) Au-(Fe₃O₄@SiO₂) and (b) (Au-Fe₃O₄)@SiO₂ nanoparticles; the average sizes detected by TEM are 30.6±3.2 and 31.5±3.5 nm, respectively. (c) Size distribution of FITC-modified Au-(Fe₃O₄@SiO₂) and (Au-Fe₃O₄)@SiO₂ in water, detected by a Malvern Nano-ZS Analyzer; the average values of hydraulic radii are 56.3 and 63.1 nm, respectively.

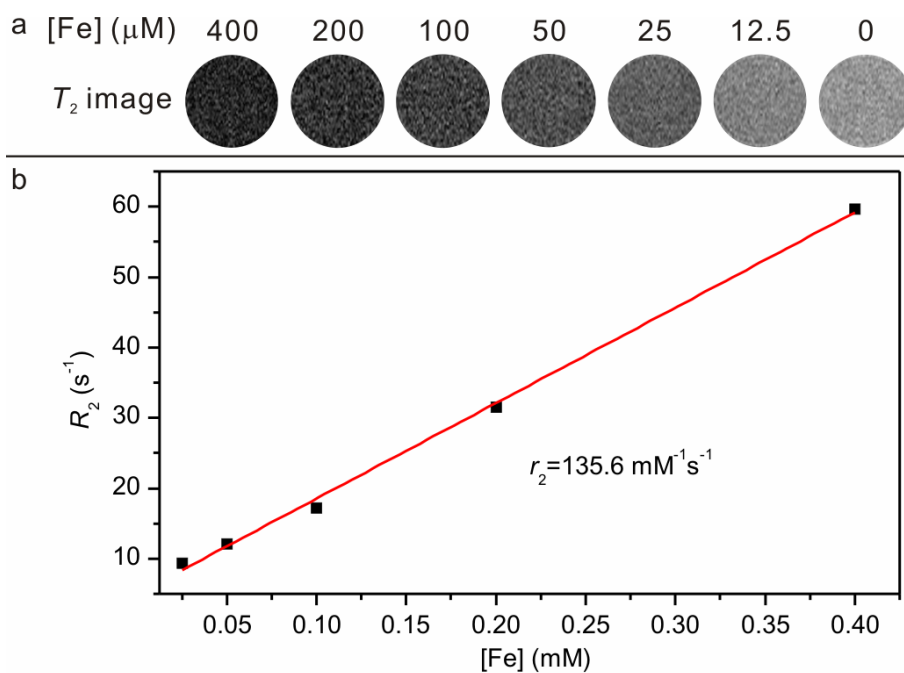


Figure S16. (a) T_2 -weighted magnetic resonance (MR) images of FITC-modified Au-($\text{Fe}_3\text{O}_4@ \text{SiO}_2$) nanoparticles at different Fe concentrations in water (containing 1% agarose gel). (b) The analysis of relaxation rate R_2 vs. Fe concentration for FITC-modified Au-($\text{Fe}_3\text{O}_4@ \text{SiO}_2$) nanoparticles in water. The relaxivity value r_2 was obtained from the slope of linear fit of experimental data. The phantom study was performed on a 0.5 T MRI scanner.

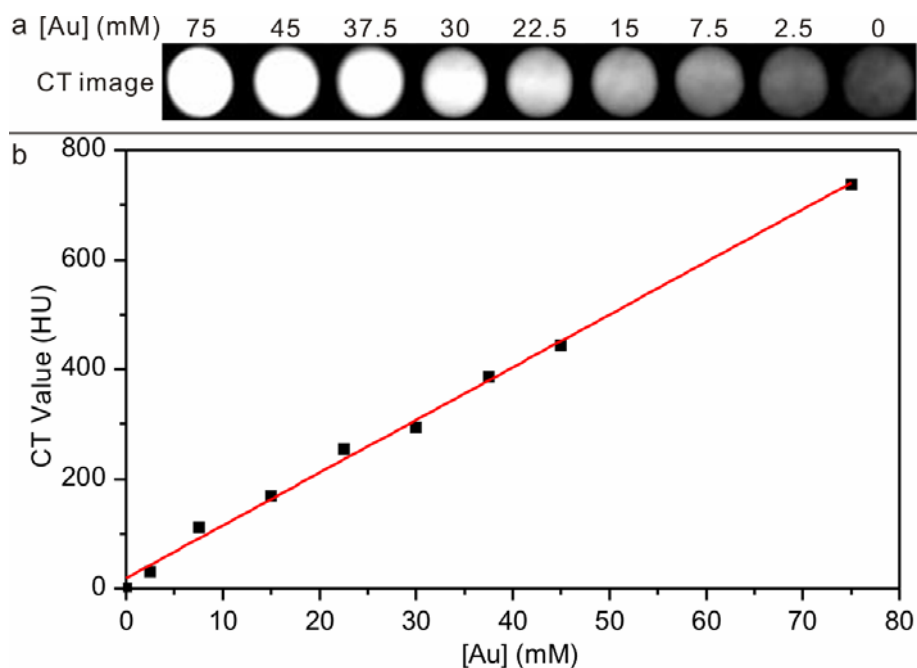


Figure S17. (a) X-ray computed tomography (CT) images of FITC-modified Au-(Fe₃O₄@SiO₂) nanoparticles with various Au concentrations *in vitro*. (b) The analysis of CT value (in Hounsfield unit, HU) vs. Au concentration for FITC-modified Au-(Fe₃O₄@SiO₂) nanoparticles in water.

References:

- S1 B. H. Wu, H. Y. Yang, H. Q. Huang, G. X. Chen and N. F. Zheng, *Chin. Chem. Lett.*, 2013, **24**, 457-462.
- S2 B. H. Wu, H. Zhang, C. Chen, S. C. Lin and N. F. Zheng, *Nano Res.*, 2009, **2**, 975-983.
- S3 Y. Han, J. Jiang, S. S. Lee and J. Y. Ying, *Langmuir*, 2008, **24**, 5842-5848.
- S4 Y. K. Park and S. Park, *Chem. Mater.*, 2008, **20**, 2388-2393.
- S5 X. Q. Huang, C. Y. Guo, L. Q. Zuo, N. F. Zheng and G. D. Stucky, *Small*, 2009, **5**, 361-365.
- S6 N. F. Zheng, J. Fan and G. D. Stucky, *J. Am. Chem. Soc.*, 2006, **128**, 6550-6551.
- S7 T. R. Zhang, J. P. Ge, Y. X. Hu, Q. Zhang, S. Aloni and Y. D. Yin, *Angew. Chem. Int. Ed.*, 2008, **47**, 5806-5811.
- S8 E. A. Vogler, *Adv. Colloid Interface Sci.*, 1998, **74**, 69-117.
- S9 Y. Tian and L. Jiang, *Nat. Mater.*, 2013, **12**, 291-292.
- S10 D. M. Andala, S. H. R. Shin, H. Y. Lee and K. J. M. Bishop, *ACS Nano*, 2012, **6**, 1044-1050.